

Photoactivable glycolipid antigens generate stable conjugates with CD1d for invariant Natural Killer T cell activation

Kharkwal, Shalu Sharma; Veerapen, Natacha; Jervis, Peter; Bhowruth, Veemal; Besra, Amareeta K; North, Simon J; Haslam, Stuart M; Dell, Anne; Hobrath, Judith; Quaid, Padraic; Moynihan, Patrick; Cox, Liam Robert; Kharkwal, Himanshu; Zauderer, Maurice; Besra, Gurdyal S; Porcelli, Steven A

DOI:

[10.1021/acs.bioconjchem.8b00484](https://doi.org/10.1021/acs.bioconjchem.8b00484)

License:

Other (please specify with Rights Statement)

Document Version

Peer reviewed version

Citation for published version (Harvard):

Kharkwal, SS, Veerapen, N, Jervis, P, Bhowruth, V, Besra, AK, North, SJ, Haslam, SM, Dell, A, Hobrath, J, Quaid, P, Moynihan, P, Cox, LR, Kharkwal, H, Zauderer, M, Besra, GS & Porcelli, SA 2018, 'Photoactivable glycolipid antigens generate stable conjugates with CD1d for invariant Natural Killer T cell activation', *Bioconjugate Chemistry*. <https://doi.org/10.1021/acs.bioconjchem.8b00484>

[Link to publication on Research at Birmingham portal](#)

Publisher Rights Statement:

Checked for eligibility: 14/08/2018

This is the accepted manuscript for a forthcoming publication in *Bioconjugate Chemistry*.

General rights

Unless a licence is specified above, all rights (including copyright and moral rights) in this document are retained by the authors and/or the copyright holders. The express permission of the copyright holder must be obtained for any use of this material other than for purposes permitted by law.

- Users may freely distribute the URL that is used to identify this publication.
- Users may download and/or print one copy of the publication from the University of Birmingham research portal for the purpose of private study or non-commercial research.
- User may use extracts from the document in line with the concept of 'fair dealing' under the Copyright, Designs and Patents Act 1988 (?)
- Users may not further distribute the material nor use it for the purposes of commercial gain.

Where a licence is displayed above, please note the terms and conditions of the licence govern your use of this document.

When citing, please reference the published version.

Take down policy

While the University of Birmingham exercises care and attention in making items available there are rare occasions when an item has been uploaded in error or has been deemed to be commercially or otherwise sensitive.

If you believe that this is the case for this document, please contact UBIRA@lists.bham.ac.uk providing details and we will remove access to the work immediately and investigate.

1
2
3 **1 Photoactivable glycolipid antigens generate stable conjugates with**
4
5
6 **2 CD1d for invariant Natural Killer T cell activation**
7
8
9 **3**

10
11 4 Natacha Veerapen^{1#}, Shalu Sharma Kharkwal^{3#}, Peter Jervis¹, Veemal Bhowruth¹,
12
13 5 Amareeta K. Besra¹, Simon J. North⁶, Stuart M. Haslam⁶, Anne Dell⁶, Judith Hobrath⁷,
14
15 6 Padraic J. Quaid¹, Patrick J. Moynihan¹, Liam R. Cox², Himanshu Kharkwal⁴, Maurice
16
17 7 Zauderer⁸, Gurdyaal S. Besra^{1*}, Steven A. Porcelli.^{3,5*}
18
19
20 8

21
22 9 ¹School of Biosciences, and ²School of Chemistry, University of Birmingham,
23
24 10 Edgbaston, Birmingham, B15 2TT, United Kingdom
25
26

27 11 ³Department of Microbiology and Immunology, ⁴Department of Developmental and
28
29 12 Molecular Biology, and ⁵Department of Medicine, Albert Einstein College of Medicine,
30
31 13 Bronx, NY, 10461, USA
32
33

34 14 ⁶Department of Life Sciences, Faculty of Natural Sciences, Imperial College
35
36 15 London, South Kensington Campus, London, SW7 2AZ, UK
37
38

39 16 ⁷Drug Discovery Unit, College of Life Sciences, University of Dundee, Dow Street
40
41 17 Dundee, DD1 5EH, Scotland, UK
42
43

44 18 ⁸Vaccinex Inc., 1895 Mount Hope Avenue, Rochester, NY 14620, USA
45
46 19

47
48 20 #These authors contributed equally to this manuscript
49

50 21 *Joint corresponding authors
51
52
53 22

1
2
3 **1 Correspondence to:**
4

5
6 **2 Steven A. Porcelli, MD**
7

8
9 **3 Department of Microbiology and Immunology**
10

11
12 **4 Forchheimer Building, Room 416**
13

14
15 **5 Albert Einstein College of Medicine**
16

17
18 **6 1300 Morris Park Avenue, Bronx, NY 10461**
19

20
21 **7 Phone: 718-430-3228. Fax: 718-430-8711**
22

23
24 **8 E-mail: steven.porcelli@einstein.yu.edu**
25

26
27
28 **9**
29

30
31 **10 Gurdyal S. Besra**
32

33
34 **11 School of Biosciences**
35

36
37 **12 University of Birmingham**
38

39
40 **13 Edgbaston, Birmingham B15 2TT, UK**
41

42
43 **14 Phone: +00 44 121 415 8125. Fax: +00 44 121 414 5925**
44

45
46 **15 E-mail: g.besra@bham.ac.uk**
47

48
49
50 **16**
51

52
53
54 **17**
55

1 **Abstract**

2
3
4
5
6 2 Activation of invariant natural killer T lymphocytes (iNKT cells) by α -galactosylceramide
7
8 3 (α -GC) elicits a range of pro-inflammatory or anti-inflammatory immune responses. We
9
10 4 report the synthesis and characterization of a series of α -GC analogues with acyl chains
11
12 5 of varying length and a terminal benzophenone. These bound efficiently to the
13
14 6 glycolipid antigen presenting protein CD1d, and upon photoactivation formed stable
15
16 7 CD1d-glycolipid covalent conjugates. Conjugates of benzophenone α -GCs with soluble
17
18 8 or cell bound CD1d proteins retained potent iNKT cell activating properties, with biologic
19
20 9 effects that were modulated by acyl chain length and the resulting affinities of
21
22 10 conjugates for iNKT cell antigen receptors. Analysis by mass spectrometry identified a
23
24 11 unique covalent attachment site for the glycolipid ligands in the hydrophobic ligand
25
26 12 binding pocket of CD1d. The creation of covalent conjugates of CD1d with α -GC
27
28 13 provides a new tool for probing the biology of glycolipid antigen presentation, as well as
29
30 14 opportunities for developing effective immunotherapeutics.
31
32
33
34
35
36
37
38
39

40 **Keywords**

41
42
43 17 CD1d, α -galactosylceramide, benzophenone, invariant Natural Killer T cells
44
45
46
47
48
49
50
51
52
53
54
55
56
57
58
59
60

1 Introduction

2 Invariant Natural Killer T (iNKT) cells are a prominent subset of unconventional T cells
3 that bridge innate and adaptive immunity to contribute to a wide range of immune
4 responses.¹ They recognize and respond to glycolipid antigens presented by CD1d, a
5 membrane protein specialized for binding and presentation of lipid antigens.² The most
6 extensively studied CD1d-presented glycolipid antigens are synthetic forms of α -
7 galactosylceramide (α -GC), which potently stimulate iNKT cell proliferation, expansion
8 and cytokine secretion.³ In mice, various structural analogues of α -GC have shown
9 impressive anti-cancer effects⁴, as well as a broad range of activities in models of
10 infection, vaccination, autoimmunity and inflammatory diseases.⁵ Thus, there has
11 been increasing interest in using α -GC analogues to develop new approaches to
12 vaccination or immunotherapy.^{4c, 6}

13 Despite the potent immune activating properties of α -GC and the
14 conservation of a CD1d-restricted iNKT cell subset in humans, there has been
15 limited success so far in translating iNKT cell-based approaches into clinical
16 applications. This may reflect problems with systemic delivery of glycolipid agonists,
17 which leads to their uptake and presentation by a wide range of cell types and the
18 stimulation of unpredictable or antagonistic immune responses.^{6a, 7}

19 Several approaches to overcoming these problems have been developed that
20 involve delivery of α -GC by antigen presenting cells (APCs) or soluble recombinant
21 CD1d proteins loaded *ex vivo* with the glycolipid.⁸ These approaches have shown
22 potential to stimulate more effective antitumor responses compared to injections of
23 free glycolipids in mouse models, as well as promising preliminary results in

1 preclinical and clinical studies.^{4c, 6a, 8c, 8d, 9} Also of note is the apparent ability of
2 these methods to induce substantial iNKT cell activation while triggering less of the
3 long-term unresponsiveness (anergy) or depletion of iNKT cells that has been a
4 problem with injections of free glycolipids.¹⁰

5 However, a potential limitation is presented by the readily reversible binding
6 of glycolipid ligands to CD1d, which is mediated by noncovalent hydrophobic and
7 hydrogen bonding interactions.² Rapid dissociation has been reported to result in
8 half-lives for α GC-CD1d complexes in some *in vitro* studies as short as a few
9 minutes or less, which may be further reduced *in vivo* by the presence of lipid
10 exchange and binding proteins.¹¹ The relatively short half-life and instability of such
11 complexes limits the duration and potency of their desirable biologic effects, and the
12 release of free glycolipids *in vivo* may contribute to unwanted effects such as iNKT
13 cell anergy or toxicities including liver damage or sensitization to endotoxic shock.¹²
14 Thus, the relative instability of α GC-CD1d complexes remains a suboptimal feature
15 in approaches that involve *ex vivo* loading of cells or CD1d proteins with glycolipids,
16 and can compromise the efficacy and precision of such controlled delivery methods.

17 In the current study, we have developed an approach to circumvent the
18 problem of glycolipid dissociation from CD1d by the use of photoactivatable forms
19 of α -GC to create covalently stabilized and highly active α GC-CD1d conjugates. A
20 series of analogues of α -GC containing a benzophenone group at the terminus of
21 their N-acyl chains was synthesized and optimized for iNKT cell stimulating activity.
22 Controlled exposure to UV irradiation generated stable covalent conjugates of these
23 glycolipids with CD1d, and these retained their ability to potently stimulate iNKT

1 cells *in vitro* and *in vivo* in mice. Specific immunologic properties such as cytokine
2 production could be modulated by variations in the size of the aliphatic chain
3 bearing the benzophenone group, which was correlated with the affinity of the
4 conjugates for the antigen receptors of iNKT cells. Mass spectrometry identified a
5 unique site for covalent bond formation in the CD1d protein, enabling detailed
6 modeling of the structure of the stable conjugates. The development of controlled
7 covalent bond formation for stabilization of α GC-CD1d conjugates provides a new
8 tool for the study of glycolipid antigen presentation, and also forms the basis for
9 improving immunotherapies based on the targeted delivery of iNKT cell activators.

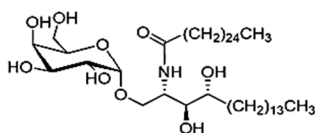
11 Results

12 Synthesis of BPGCs

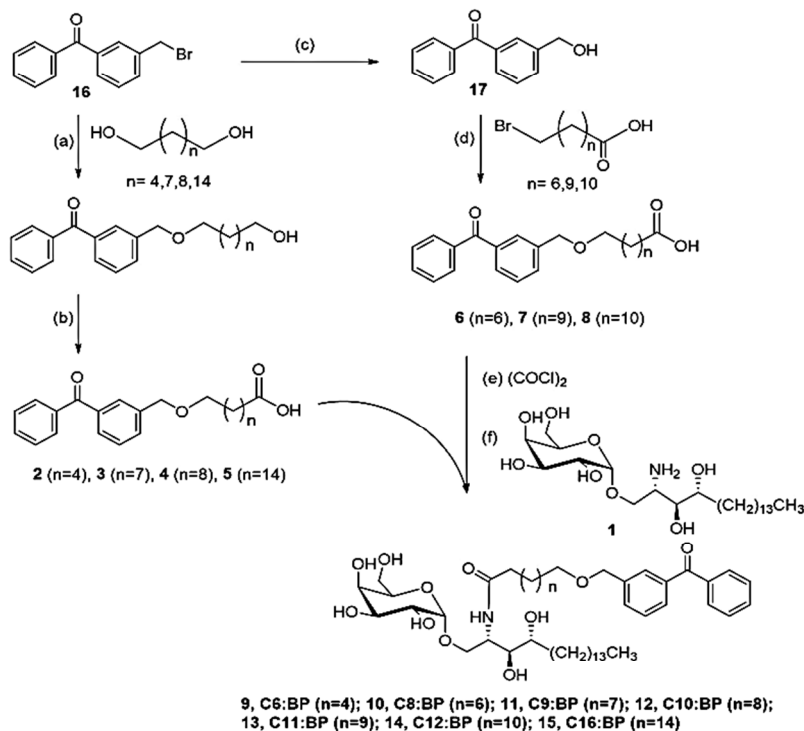
13 Extensive previous work has shown that many modifications of the fatty acyl chain of
14 α -GC can be tolerated without disruption of glycolipid binding to CD1d or loss of iNKT
15 cell stimulating activity³, consistent with the large volume of the hydrophobic ligand
16 binding site of CD1d.^{2, 13} Thus, we developed a synthetic strategy for introduction of a
17 photoactivatable moiety on the acyl chain terminus of α -GC to enable the controlled
18 formation of a covalent bond between the glycolipid and the CD1d protein (**Fig. 1**). The
19 benzophenone group was chosen as it can be activated by UV irradiation to give the
20 corresponding benzhydryl biradical, which we postulated would react with a proximal
21 C-H bond present in the CD1d protein to form a permanent covalent bond. A group of
22 benzophenone-containing derivatives of α -GC (BPGCs) bearing acyl chains of various
23 lengths (compounds **9-15**) were synthesized to determine which would optimally

1 associate with CD1d and effectively activate iNKT cells. Based on the resemblance of
 2 benzophenone to a C10 isoprene unit, we synthesized a range of BPGCs which mimic
 3 *N*-acyl chain lengths from C16 (C6:BP (**9**)) to C26 (C16:BP (**15**)), thus spanning the
 4 range found in most highly active α -GC analogues.³ These compounds were readily
 5 prepared via acylation of the parent compound **1** with carboxylic acids (**2-8**), following
 6 their conversion to the corresponding acid chlorides using oxalyl chloride. Ensuing
 7 acylation of the amine **1** in a 1:1 mixture of THF and saturated sodium acetate solution
 8 afforded the benzophenone-derivatised glycosphingolipids (BPGCs) **9-15** (Fig. 1).

a



b



9

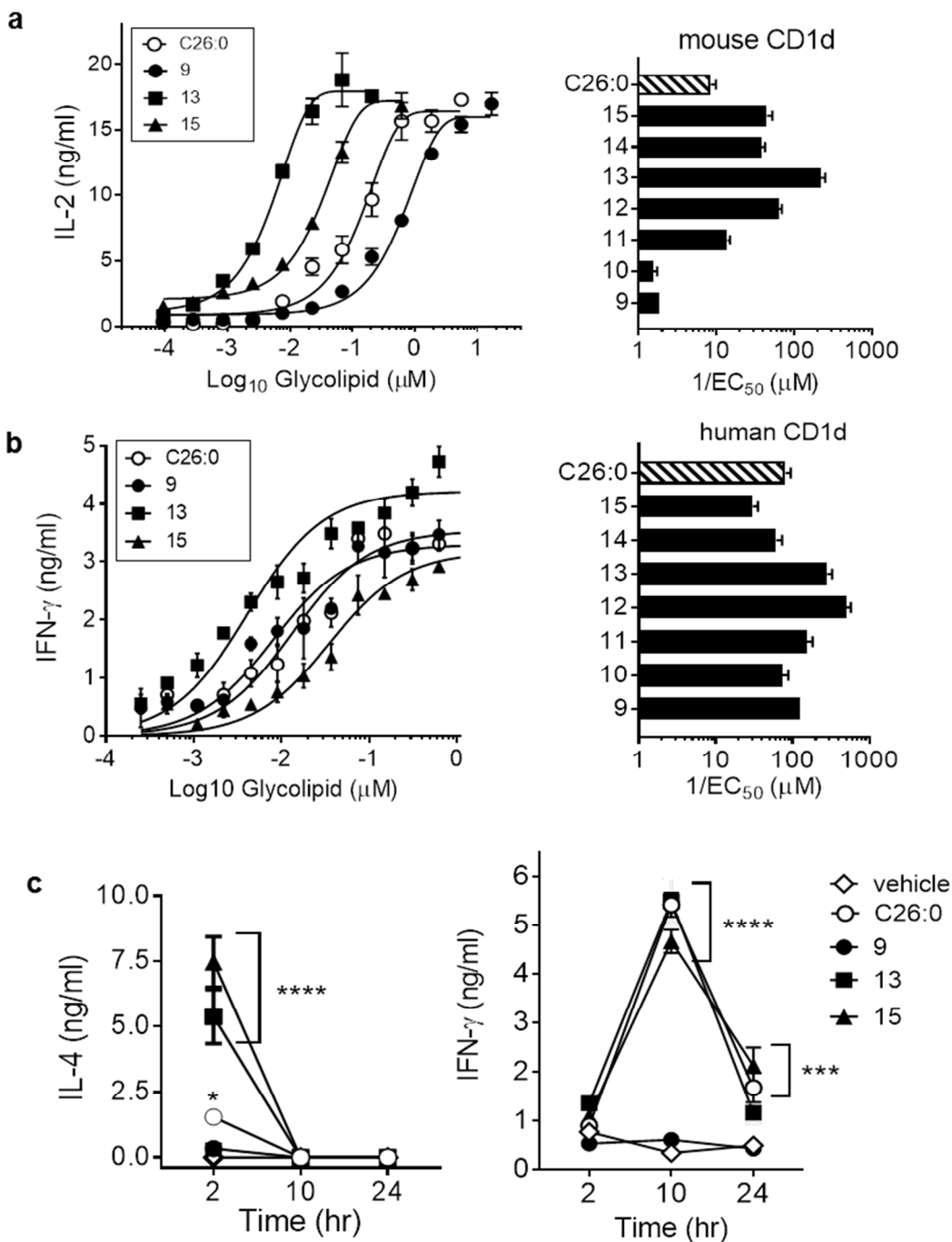
1
2
3 **Figure 1: Synthesis of BPGCs.** (a) Structure of the prototypical iNKT cell activating
4 glycolipid, α -GC C26:0. (b) General scheme for synthesis of BPGCs with acyl group
5 spacers of varying length (compounds **9 – 15**). (a) NaH, DMF, 0 °C to rt; (b) PDC, wet
6 THF, rt; (c) CaCO₃, THF, H₂O, 100 °C, 12 h; (d) NaH, DMF, 0 °C to rt; (e) (COCl)₂, 60
7 °C, 2 h; (f) NaOAc, THF, rt, 12 h. Incorporation of the benzophenone group into
8 carboxylic acids was accomplished through the use of a flexible ether linkage to allow
9 rotational freedom and optimal orientation of the aromatic group in the CD1d ligand-
10 binding pocket. To synthesize carboxylic acids (**2-8**), we used a versatile strategy
11 involving an S_N2 displacement of a bromide using various diols and 3-
12 (bromomethyl)benzophenone (**16**) or through a variety of bromocarboxylic acids by 3-
13 (hydroxymethyl)benzophenone (**17**). The monoalkylation of the diols with 3-
14 (bromomethyl)benzophenone (**16**), which was obtained using published procedures¹⁴,
15 was achieved in reasonable yields by using the diols in excess. Oxidation of the
16 corresponding alcohols to the acids with pyridinium dichromate (PDC) was sluggish and
17 only afforded compounds **2-5** in average yields. In contrast, alkylation of the alcohol **17**
18 with the bromocarboxylic acids in DMF and sodium hydride as base proceeded
19 smoothly to afford the desired carboxylic acids **6-8** in quantitative yields (see
20 Supplemental Information for further details of synthesis and characterization).
21
22
23
24
25
26
27
28
29
30
31
32
33
34
35
36
37
38

20 **Stimulation of iNKT cells by BPGC analogs**

39 A variety of *in vitro* biological assays were performed to assess the iNKT cell activating
40 properties of the BPGCs upon presentation by CD1d, and to determine the effect of the
41 varying acyl chain lengths and the presence of a bulky terminal benzophenone group on
42 their biologic activities. A standard assay using co-culture of mouse bone marrow-
43 derived dendritic cells (BMDCs) and a murine iNKT cell hybridoma was used to assess
44 the activity and relative potencies of BPGCs (**Fig. 2a**).¹⁵ This showed significant iNKT
45 cell stimulating activity for all BPGCs tested, with a substantial impact of the length of
46 fatty acyl chain. Optimal iNKT stimulation in the mouse cell culture system was
47
48
49
50
51
52
53
54
55
56
57
58
59
60

1
2
3 1 achieved with **13**, which along with several other BPGCs was significantly more potent
4
5 2 than the standard α -GC (C26:0), which is generally considered a highly potent iNKT cell
6
7 3 activator both *in vitro* and *in vivo*.^{4a, 15} A similar *in vitro* analysis was carried out using a
8
9 4 canonical human iNKT cell clone co-cultured with HeLa cells transfected to express
10
11 5 human CD1d (**Fig. 2b**).¹⁶ This also revealed strong activity of BPGCs as measured by
12
13 6 IFN- γ secretion, which was similar to or greater than that stimulated by C26:0. As for
14
15 7 the mouse culture system, compounds **12** and **13** showed the greatest potency in this
16
17 8 assay, although length of the fatty acyl tail had much less apparent impact in the human
18
19 9 system.

20
21
22
23
24 10 To directly assess activity *in vivo*, we analyzed serum cytokine levels following
25
26 11 intravenous injection of selected BPGCs. For this analysis, we tested **9** which was a
27
28 12 relatively weak activator of murine iNKT cells *in vitro*, and **13** and **15** which were more
29
30 13 potent than C26:0 in both mouse and human cell culture assays. Mice were injected
31
32 14 with 4 nmoles of each glycolipid and bled after 2, 10 and 24 hours to quantitate serum
33
34 15 IFN- γ and IL-4, as previously described.¹⁵ Significant levels above baseline for serum
35
36 16 IL-4 were detected with **13** and **15** at two hours, which declined to undetectable levels
37
38 17 by 10 hours (**Fig. 2c**). The IL-4 levels were several fold higher for **13** and **15** compared
39
40 18 to C26:0, indicating a rapid and powerful activation of iNKT cells. Consistent with this,
41
42 19 IFN- γ levels showed a sustained rise with **13** and **15** with a peak at 10 hours that closely
43
44 20 resembled the response to C26:0, while **9** did not stimulate detectable levels above
45
46 21 background for either cytokine tested. Thus, BPGCs retained their iNKT cell activating
47
48 22 properties *in vivo*, and the potencies of different analogues varied depending on the
49
50 23 length of their acyl chains.



1
2
3
4
5
6
7
8
9
10
11
12
13
14
15
16
17
18
19
20
21
22
23
24
25
26
27
28
29
30
31
32
33
34
35
36
37
38
39
40
41
42
43
44
45
46
47
48
49
50
51
52
53
54
55
56
57
58
59
60

Figure 2: iNKT stimulatory activity of BPGCs. (a) Responses of mouse iNKT cell hybridoma DN3A4-1.2 cultured with bone marrow derived dendritic cells from C57BL/6 mice and the indicated concentrations of BPGCs or α -GC C26:0. IL-2 secretion was measured in supernatants after 18 hours of culture. Representative dose-response curves are shown on the left for three of the seven BPGCs and standard α -GC C26:0.

1
2
3 1 Concentrations stimulating 50% of the maximum response (EC_{50}) were determined for
4 each glycolipid, and reciprocal values are plotted on the right. (b) Similar analysis as in
5 2 each glycolipid, and reciprocal values are plotted on the right. (b) Similar analysis as in
6 3 (a) except using human iNKT clone HDE3 and HeLa cells expressing human CD1d with
7 4 measurement of secreted IFN γ as the readout for activation. (c) *In vivo* activities of **9**,
8 5 **13** and **15** were determined by quantitating serum IL-4 and IFN- γ 2, 10 and 24 hours
9 6 post glycolipid injection. Peak values for serum IL4 (left) and IFN- γ (right) were found at
10 7 2 and 10 hours respectively.

11 8 All symbols and bars are means for triplicate samples, and error bars are ± 1 SD. * P <
12 9 0.05, ** P < 0.01, *** P < 0.001, **** P < 0.0001 for comparisons to vehicle treated mice
13 10 (two-way ANOVA with Dunnett's multiple comparison test). All data are representative
14 11 of at least three separate experiments.

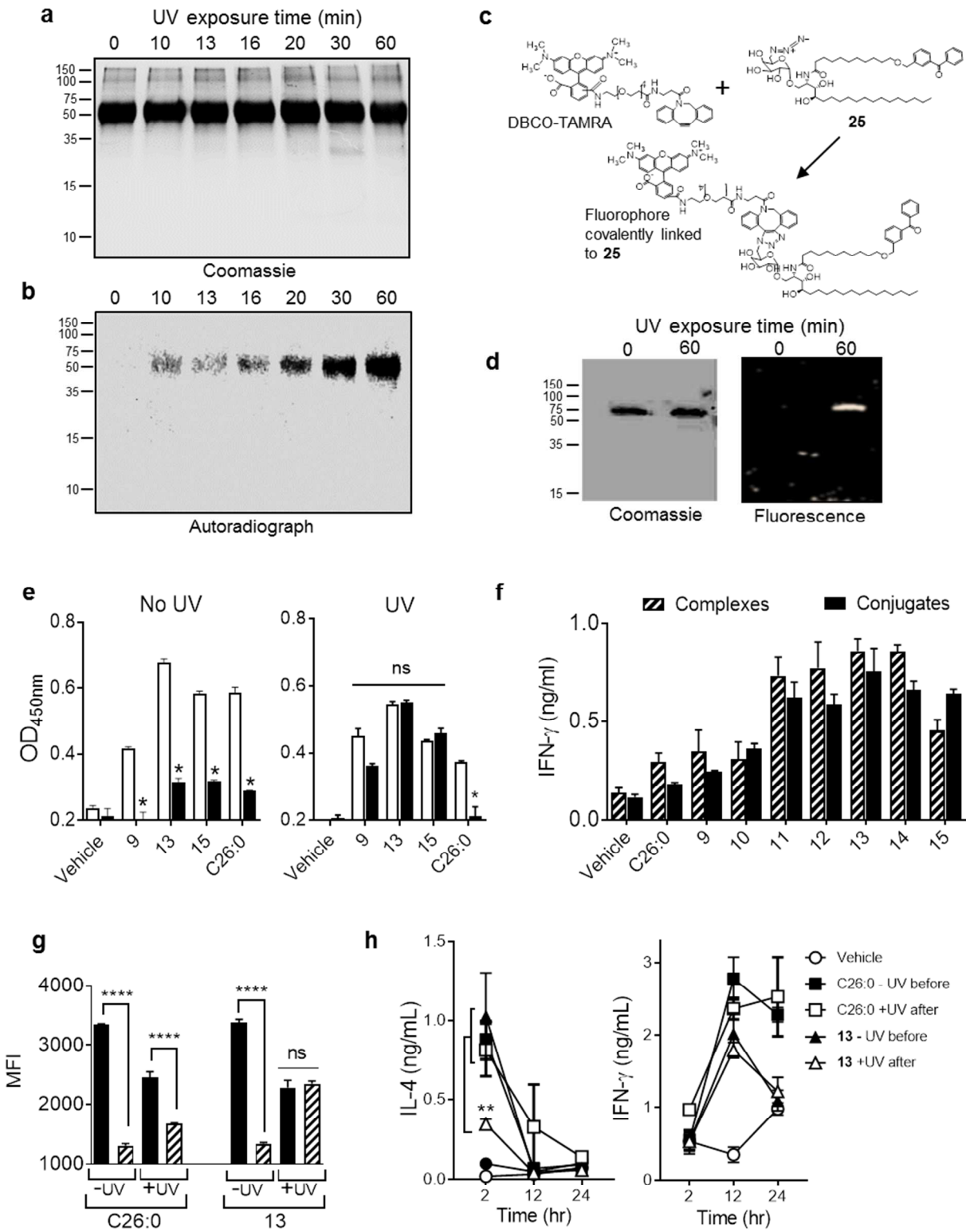
15 12

16 13 **Formation of covalent CD1d-glycolipid conjugates by photoactivation**

17 14 The known photochemical properties of benzophenones predicted that loading of
18 15 BPGCs into CD1d proteins followed by exposure to UV irradiation should form
19 16 covalently stabilized protein-glycolipid conjugates. We validated this initially using a 3-
20 17 fold molar excess of ^{14}C -labelled analogue of **13**, compound **26** (Scheme 2, SI) to load
21 18 soluble recombinant mCD1d protein. Aliquots of the loaded protein were then exposed
22 19 to a 365 nm UV lamp for times ranging from 0 to 90 minutes, followed by denaturation
23 20 (1% SDS at 100° C for 5 min) and separation by SDS-PAGE. Staining of the gel with
24 21 Coomassie blue revealed intact protein in all samples, which ran at the predicted size of
25 22 ~57 kDa for monomeric soluble CD1d (**Fig. 3a**). Autoradiography of the same gel
26 23 revealed the presence of the ^{14}C label co-migrating with CD1d protein in the samples
27 24 exposed to UV light, but not in the unexposed sample (**Fig. 3b**). Maximum association
28 25 of radiolabel, indicating the formation of stable protein-glycolipid conjugates that were
29 26 resistant to denaturation, was achieved following 30 to 60 minutes of UV exposure,

1
2
3 1 corresponding to a delivered dose range of 400 – 600 mJoules/cm². Radiometric
4
5 2 analysis showed that approximately 70% of CD1d molecules were conjugated to ¹⁴C
6
7 3 labeled **26** after 60 minutes of UV exposure (**Supplemental Figure S1**).
8
9
10
11
12
13
14
15
16
17
18
19
20
21
22
23
24
25
26
27
28
29
30
31
32
33
34
35
36
37
38
39
40
41
42
43
44
45
46
47
48
49
50
51
52
53
54
55
56
57
58
59
60

1



2

1
2
3 **Figure 3: Covalent conjugation of BPGCs to mCD1d.** (a) Coomassie stained gel
4 and (b) autoradiograph of denaturing SDS-PAGE after exposing mCD1d: ^{14}C -labelled
5 analogue of **13**, compound **26** (Scheme 2, SI) complexes (~57 kDa) for various lengths
6 of time. (c) Diagrammatic representation of click reaction of DBCO-TAMRA dye with
7 azide-linked-**25** (SI) either loaded non-covalently or covalently conjugated to CD1d
8 protein. (d) Coomassie stained and fluorescent images of denaturing SDS-PAGE gel of
9 fluorescently tagged noncovalent-complexes (0 min UV exposure) and covalent-
10 conjugates (60 min UV exposure) of mCD1d fusion protein (~78 kDa). (e) Complexes
11 (No UV, left) or conjugates (UV, right) loaded with the indicated BPGC or α -GC-C26:0
12 were coated on high binding plates and incubated for 3 days at room temperature either
13 without (white bars) or with (black bars) washing twice per day with PBS + 0.1% Triton
14 X-100. Residual glycolipid binding to mCD1d was detected by ELISA using biotinylated
15 monoclonal antibody L363. * $P < 0.001$ for multiple t tests of comparisons of washed
16 versus unwashed samples with each glycolipid. (f) Splenocytes (2×10^5 per well in 0.2
17 ml complete medium) were stimulated *in vitro* for 18 hours with complexes (hatched
18 bars) and conjugates (solid bars) immobilized on high binding plates. Supernatants
19 were collected and assayed for IFN- γ by ELISA. (g) JAWS II cells (5×10^4 per well)
20 pulsed overnight with 100 nM glycolipids (C26:0 or **13**) were either exposed to UV (~400
21 mJ/cm 2) or left untreated. Cells were stained with L363-AlexaFluor647 either directly
22 (solid black bars) or after multiple washes (hatched bars) to allow dissociation and
23 analyzed by flow cytometry. **** $P < 0.0001$, two-way ANOVA with Bonferroni correction
24 for indicated comparisons. (h) JAWS II cells were exposed to UV (600 mJ/cm 2) either
25 before (black symbols) or after (white symbols) pulsing with vehicle, C26:0 or **13** at 100
26 nM concentration. Cells were washed thrice during 24 hours of incubation and
27 adoptively transferred i.v. into mice (3×10^5 cells per mouse, 4 mice per group). Blood
28 samples were obtained after 2, 12 and 24 hours to quantitate serum IL-4 and IFN- γ . ** P
29 < 0.01 , two-way ANOVA with Bonferroni correction for indicated comparisons. Data
30 plotted in (e) – (f) are shown as means for a minimum of three replicates, and error bars
31 are ± 1 SD. All experiments were performed at least three times.

1
2
3 1 Further analysis of conjugate formation was carried out in studies using
4
5 2 compound **25** (synthesis described in SI), an analogue of **13** carrying an azido group at
6
7 3 the 6'- position of the saccharide head group (**Fig. 3c**). Complexes formed between this
8
9 4 glycolipid and soluble mCD1d were either irradiated with UV λ 365 or not, and then
10
11 5 incubated with fluorescent DBCO-TAMRA, which reacts with the azido group of the
12
13 6 glycolipid.¹⁷ The samples were then denatured and analyzed by SDS-PAGE. While
14
15 7 gels stained with Coomassie blue showed similar CD1d protein in both samples
16
17 8 (migrating at ~78 kDa, consistent with the mCD1d fusion protein used for this
18
19 9 experiment; see Online Methods for details), only the sample exposed to UV had a
20
21 10 fluorescent signal co-migrating with CD1d (**Fig. 3d**). This confirmed the formation of
22
23 11 stable conjugates following photoactivation of the benzophenone moiety in CD1d-
24
25 12 glycolipid complexes. In addition, the ability of the DBCO-TAMRA reagent to couple to
26
27 13 the azido group was consistent with correct orientation of the **13** in the CD1d lipid
28
29 14 binding groove, with the carbohydrate head-group exposed and accessible at the
30
31 15 surface of the protein.

32
33
34
35
36
37 16 To confirm the correct conformation and stability of covalent mCD1d-BPGC
38
39 17 conjugates, we tested reactivity with mAb L363, which binds specifically to CD1d loaded
40
41 18 with α -GC in a manner that closely mimics the TCRs of iNKT cells.¹⁸ Plate immobilized
42
43 19 mCD1d proteins were loaded with BPGCs, then either UV irradiated or not and tested
44
45 20 for binding of L363. This showed binding to levels comparable to that with C26:0
46
47 21 loaded mCD1d (**Fig. 3e**). Furthermore, after repeated washing with buffer containing
48
49 22 mild detergent to remove reversibly bound glycolipids, we observed significant loss of
50
51 23 L363 binding in samples without UV irradiation. In contrast, UV exposed samples
52
53
54
55
56
57
58
59
60

1 loaded with BPGCs showed no significant loss of L363 binding, indicating covalent bond
2 formation. As expected, L363 binding to mCD1d loaded with C26:0 was reversible
3 under these conditions with or without UV exposure. To further characterize the
4 biologic activity of these complexes or conjugates, we also assessed their ability to
5 stimulate iNKT cell activation in mouse splenocytes (**Fig. 3f**). The UV treated stable
6 conjugates retained their iNKT cell stimulating activity at levels comparable to
7 noncovalent complexes, indicating that UV exposure and covalent bond formation did
8 not adversely alter TCR recognition. Analysis of all seven BPGCs in this assay showed
9 an influence of the acyl chain spacer length on potency of stimulation, with **13** generally
10 showing the strongest stimulation.

11 In addition to the analyses of loading and photo-crosslinking to purified
12 recombinant CD1d proteins, we also assessed the formation of stabilized mCD1d-
13 glycolipid conjugates on intact CD1d-expressing antigen presenting cells. We used the
14 murine immortalized dendritic cell line JAWS II for this, since it expresses mCD1d and is
15 capable of glycolipid antigen presentation.¹⁹ Incubation of these cells with either C26:0
16 or **13** generated strong surface staining with mAb L363, which for both glycolipids was
17 greatly reduced following incubation for 1 day in the absence of the glycolipids. In
18 contrast, exposure of the cells to UV irradiation following culture with the **13** eliminated
19 any loss of L363 staining with subsequent culture, whereas UV irradiation of C26:0
20 loaded cells did not prevent decay of L363 binding under the same conditions (**Fig. 3g**).
21 This strongly suggested that stabilized covalent CD1d-glycolipid conjugates were
22 produced by UV photoactivation of BPGCs in living cells. This was further evaluated by
23 testing the ability of JAWS II cells loaded with **13** and UV treated to stimulate iNKT cell

1
2
3 1 responses *in vivo* following adoptive transfer of the cells into mice (**Fig. 3h**). We
4
5 2 detected strong serum cytokine responses in mice receiving cells bearing the putative
6
7 3 covalently stabilized conjugates, and a reduced level of IL-4 relative to IFN- γ was
8
9 4 observed when compared to injection of cells presenting noncovalent complexes (i.e.,
10
11 5 JAWS II cells without UV photoactivation or loaded with C26:0).
12
13 6

7 **Impact of conjugation on TCR affinity and biologic activity *in vivo***

8 By eliminating dissociation of glycolipid binding to CD1d, we anticipated that conjugation
9
10 9 should increase the overall affinity of cognate interactions with iNKT cell TCRs. To
11
12 10 assess this, fluorescent tetramers of soluble mCD1d loaded with C26:0 or BPGCs were
13
14 11 prepared with and without covalent crosslinking. Binding avidities of tetramers to the
15
16 12 TCRs of mouse iNKT cell hybridoma line DN3A4-1.2 were quantified by measuring
17
18 13 equilibrium binding to the cells over a range of concentrations, as previously
19
20 14 described.¹⁵ Extrapolation of the equilibrium dissociation constant (K_D) values showed
21
22 15 maximum avidities for C26:0 and **15** loaded noncovalent complexes, while avidities
23
24 16 declined progressively for BPGCs with shorter acyl tail spacers (**Fig. 4a**). This trend
25
26 17 was not evident with the binding of covalent conjugate tetramers, as the conjugates with
27
28 18 shorter acyl chain variants of BPGCs showed enhanced and more uniform avidities.
29
30 19 These results indicated that dissociation of the glycolipids with shorter acyl tails had a
31
32 20 major impact in TCR avidity, which was reversed by covalent stabilization of the
33
34 21 glycolipid-protein interaction. One apparent exception was the **9** conjugate, which
35
36 22 showed a distinctly lower TCR avidity than the other conjugates tested despite covalent
37
38 23 stabilization.

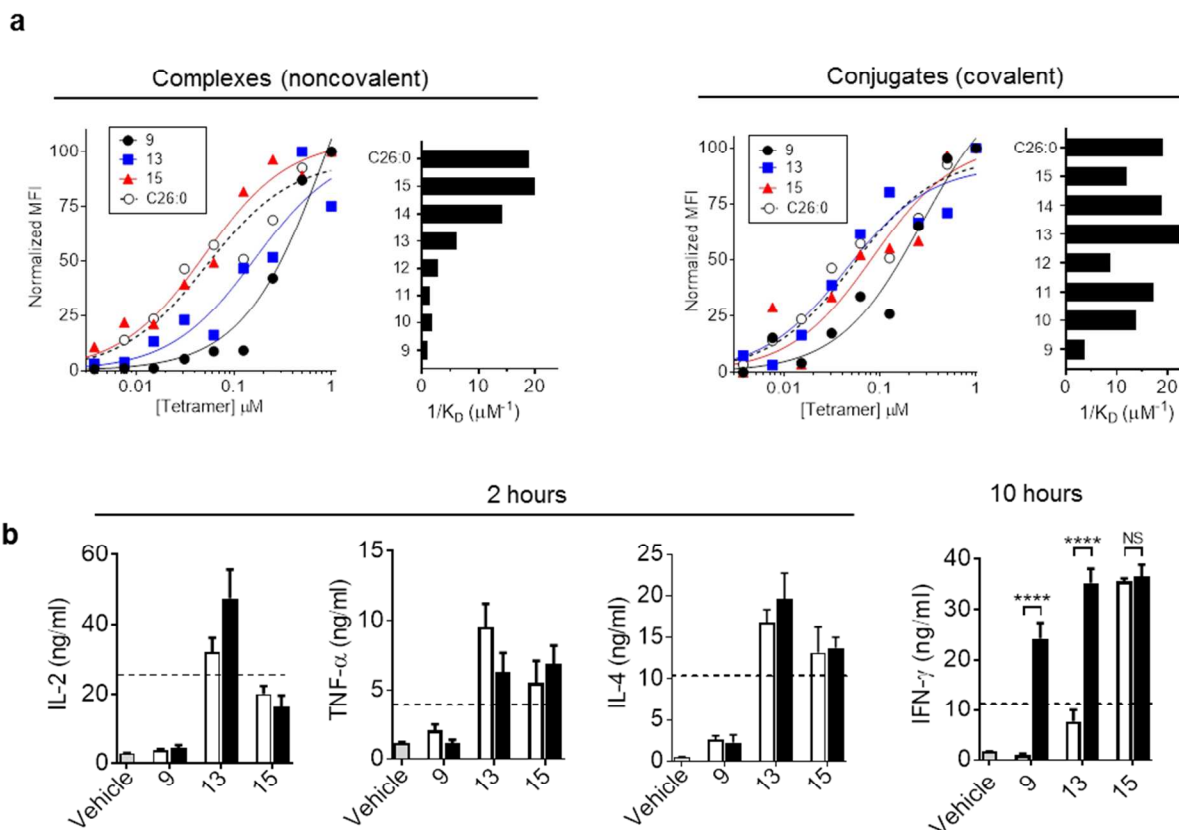


Figure 4: Affinity for iNKT cell TCR and effects on cytokine profiles. (a)

Equilibrium binding of mCD1d tetramers loaded with BPGCs over a range of tetramer concentrations was used to assess avidities of complexes (not UV irradiated, left) and conjugates (UV irradiated, right) for TCRs of mouse iNKT cell hybridoma DN3A4-1.2.

Cells stained with tetramers for 1 hour at room temperature were analyzed by flow cytometry. Normalized representative binding curves are shown for three BPGC loaded tetramers, and for standard C26:0 loaded tetramers (not UV irradiated) for comparison (dashed lines). Bar graphs show reciprocal of K_D values ($1/EC_{50}$) to summarize results for all tetramers.

(b) Serum cytokine levels following i.v. injection of mice with complexes (open bars) or conjugates (filled bars) loaded with the indicated BPGCs. Serum levels are shown at 2 hours post injection for IL-2, TNF- α and IL-4, and at 10 hours for IFN- γ . Background levels of cytokines in sera from mice injected with inert aqueous vehicle (gray bars), and levels for mice injected with 4 nmoles of free C26:0 glycolipid (horizontal dashed lines) are shown for reference. Bars represent means for groups of 4 animals each, and error bars show 1 SD. **** $P < 0.0001$ for conjugate

1
2
3 1 versus complex in the indicated comparisons (2-way ANOVA with Bonferroni's multiple
4 2 comparisons test). NS, not significant ($P > 0.05$). Differences were not significant for
5 3 other comparisons shown between complexes and conjugates.
6
7
8
9 4

10 5 We next assessed the *in vivo* activities of soluble mCD1d-BPGC complexes and
11 6 conjugates using three different BPGCs that varied in their affinities for iNKT cell TCRs.
12 7 After a single i.v. injection of mCD1d complexes or conjugates loaded with **9**, **13** or **15**
13 8 (30 μg of mCD1d protein containing ~ 0.4 nmoles of each glycolipid), serum levels of IL-
14 9 2, TNF- α , IL-4 and IFN- γ were determined at 2, 10 and 24 hours after administration
15 10 (**Fig. 4b, and Supplemental Fig. S2**). Injection of C26:0 as a free glycolipid was used
16 11 as a standard which is known to activate iNKT cell-dependent release of various
17 12 cytokines, such as IL-2, TNF- α and IL-4 which peak in serum at approximately 2 hours,
18 13 and IFN- γ which peaks at 10-12 hours after the injection.²⁰ The administration of
19 14 conjugates formed with **13** or **15** activated secretion of all four cytokines, including
20 15 levels of IL-2, TNF- α and IL-4 at 2 hours and IFN- γ at 10 hours, that equaled or
21 16 exceeded those stimulated by free C26:0. Noncovalent complexes gave similar
22 17 stimulation as conjugates at 2 hours, but the level of IFN- γ at 10 hours was significantly
23 18 higher with conjugates for **13**, and also for conjugates with **9** which did not stimulate any
24 19 detectable serum cytokines at 2 hours. These findings confirmed the iNKT cell
25 20 activating properties of soluble complexes and conjugates *in vivo*, and also were
26 21 consistent with the ability of covalent conjugation to stabilize the shorter **9** and **13**
27 22 glycolipids, extending the duration of their bioactivity. In addition, covalently stabilized **9**
28 23 conjugates showed a remarkable skewing of the cytokine response such that only IFN- γ
29 24 was detected among the cytokines measured.
30
31
32
33
34
35
36
37
38
39
40
41
42
43
44
45
46
47
48
49
50
51
52
53
54
55
56
57
58
59
60

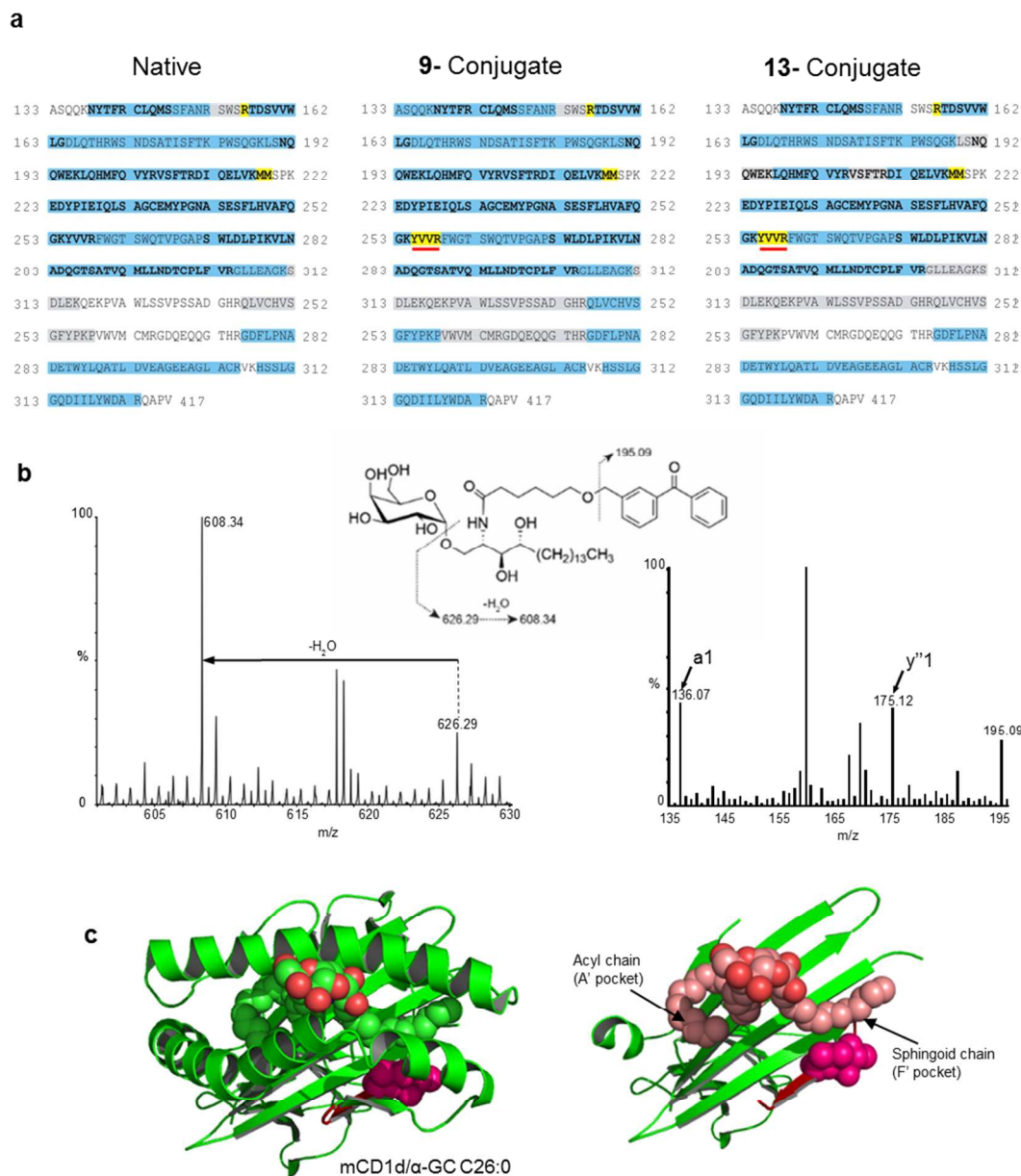


Figure 5: Mapping of covalent attachment site. (a) Peptide mapping summaries from nano-LC-ES-MS^E analyses are shown for unloaded mCD1d fusion protein (native) and for protein-glycolipid conjugates containing either **9** or **13**, focusing on the lipid binding region comprising the α 1 and α 2 regions of CD1d. Amino acid sequences of mCD1d α 1 through α 2 domains are shown in single letter code. Bold text indicates residues forming the lipid binding pocket, blue shading indicates residues mapped with a high degree of confidence, and grey shading indicates residues mapped with a good degree of confidence. Residues highlighted in yellow indicate amino acids that were not

1
2
3 1 observed in any detected peptides. Peptides containing the four amino acids
4 underlined in red in both conjugates were detected with high confidence in the native
5 protein but, were absent in both conjugates. (b) MS^E analysis of the doubly charged ion
6 m/z 661.33 observed at 30.9 min elution time in the analysis of a reduced,
7 carbamidomethylated, PNGase-F treated tryptic digest of the **9** conjugate. The
8 molecular ion is consistent with the tryptic peptide containing the ²⁵⁵YVVR₂₅₈ residues
9 modified by a single C6 glycolipid moiety. Labelled ions in the left panel show loss of
10 water from a cleaved C6 BPGC entity, while the right panel highlights evidence for the
11 peptide with the y''1 ion for the C-terminal arginine at m/z 175 and the a1-ion for the N-
12 terminal tyrosine at m/z 136. The ion at m/z 195 is consistent with loss of the
13 benzophenyl group from the BPGC molecule. (c) The mCD1d protein structure
14 previously deduced from X-ray crystallography (PDB number 3HE6) is shown as a
15 ribbon diagram in green, and the two valine residues comprising the proposed covalent
16 attachment site are shown as bright pink spheres. The view on the left shows the intact
17 α1 and α2 domains with α-GC C26:0 (green and red spheres) bound in the lipid binding
18 groove. In the view on the right, the α-helices forming the roof of the groove have been
19 removed, and the bound glycolipid is shown as pink and red spheres.

19 **Analysis of conjugation site by peptide mapping**

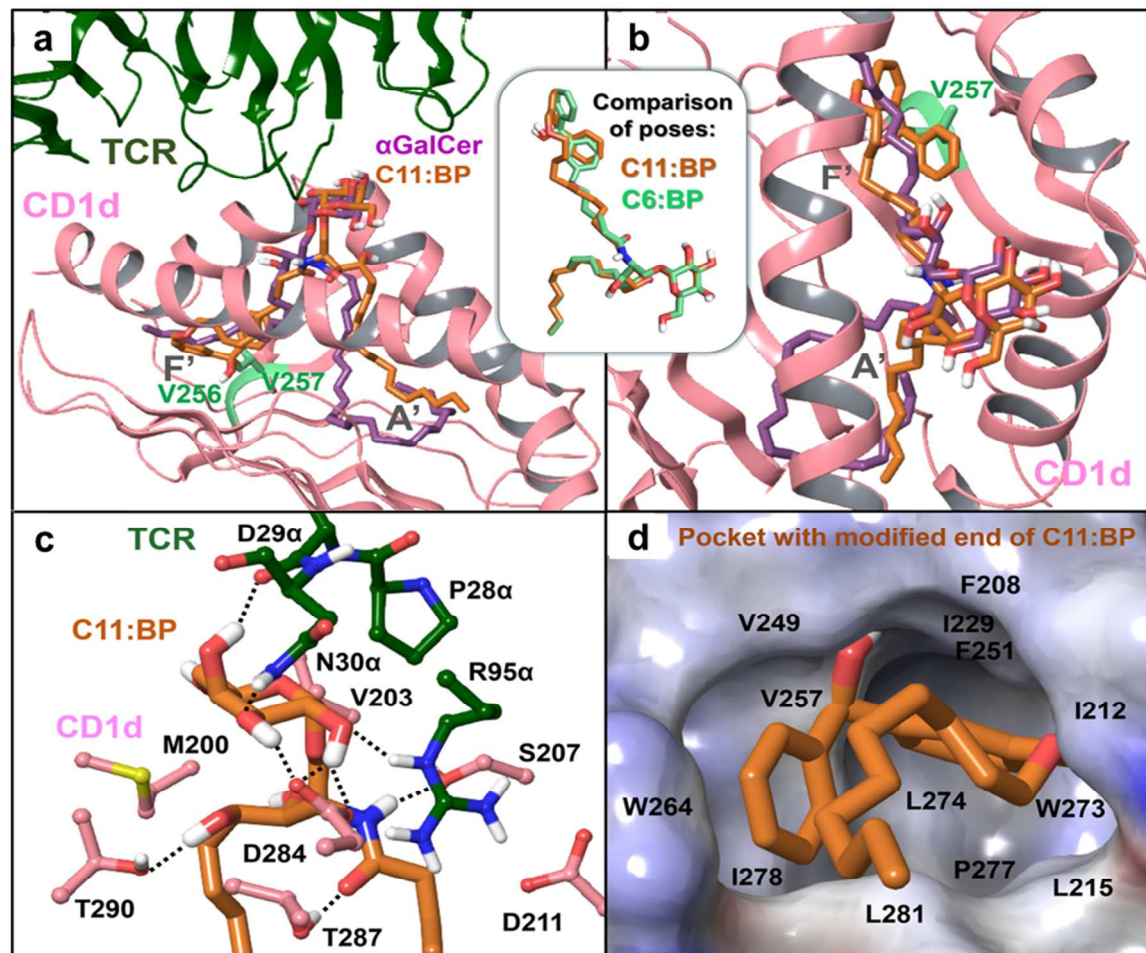
20 Peptide mapping analyses of samples of native mCD1d and mCD1d conjugates with **9**
21 and **13** were performed to identify possible sites of conjugation. Samples with or without
22 enzymatic deglycosylation were digested with trypsin, or with trypsin plus chymotrypsin.
23 Digested samples were analysed by online nano-liquid chromatography-electrospray
24 tandem mass spectrometry (nano-LC-ES-MS^E) (**Supplemental Fig.S4**). For native
25 mCD1d samples, peptides covering the entirety of the glycolipid binding domains were
26 consistently mapped with a high degree of confidence for all but three residues (R156,
27 M218 and M219) of the putative binding site. Both the **9** and **13** conjugated samples
28 produced very similar data to that of the native mCD1d, with the notable exception that

ions covering the unmodified region ${}_{255}\text{YVVR}_{258}$ were not observed (**Fig. 5a**, and **Supplemental Tables S1 – S3**). Instead, molecular ions consistent with the presence of a **13** or **9** modification were detected (**Supplemental Figures S4 and S5**), and fragmentation of these modified peptides produced signals corresponding to both the *N*-terminal tyrosine and the C-terminal arginine, as well as *y*'- and *b*-ions consistent with modified VVR and YVV (**Fig. 5b**). Although definitive evidence for covalent modification of a specific residue was not obtained, these data strongly supported the site of conjugation to be in the region ${}_{255}\text{YVVR}_{258}$, with one or both valine residues at the base of the F' pocket of mCD1d being directly involved in the formation of potential bioconjugation products (**Fig. 5C and Supplemental Fig. S6**).

12 **Modelling BPGC analogue binding modes.**

To confirm the feasibility of the putative conjugation site identified in mCD1d, the binding modes of **9** and **13** were modelled into the published crystal structure of the ternary complex of CD1d with α -GC C26:0 and the $V\alpha 14$ - $V\beta 8.2$ iNKT cell TCR (PDB entry code 3HE6) (**Fig. 5c and Fig. 6**). Briefly, compound **13** was docked without its benzophenone group, which was deleted prior to docking. The binding of the modified benzophenone group (i.e., diphenylmethanol, formed by the benzophenone group after conjugation) was predicted in a separate docking run considering that the flexible linker in the BPGC analogues would only minimally restrain possible binding conformations of the end group. The most favorable docking pose showed excellent shape complementarity and non-polar contacts in the binding site while linked covalently to the V257 side chain in the F' pocket. The diphenylmethanol pose and the sugar moiety of

1 **13** docked without the benzophenone end group were then connected by predicting an
 2 optimal conformation for the flexible linker between them through docking the linker
 3 segment (with constraints). Models of the full **9** and **13** structures were generated
 4 through splicing in the appropriate linkers of the two BPGC analogues, and were then
 5 refined using Prime complex structure refinement in Schrödinger software (**Fig. 6**).



6
 7 **Figure 6: Molecular docking of 13 and 9 in mCD1d.** (a, b) Two views of the
 8 binding model of **13** and co-crystallized α -GC (from PDB code 3HE6). The inset
 9 compares the binding models of **13** (C11:BP) and **9** (C6:BP). The modified end in the
 10 F' pocket is covalently attached to V257 (residue V125 in the structure with PDB code
 11 3HE6). (c) Interactions near the sugar moiety of **13**. A TCR interaction shared between
 12 α -GC C26:0 in the crystal structure and both **9** and **13** models was the hydrogen-

1 bonding interaction of the galactose 3''-OH with N30 α . Additional stabilizing interactions
2 with the sugar moiety of the bound BPGCs included hydrogen bonds with TCR residues
3 R95 α and D29 α and with D284 of mCD1d. The binding site that in the crystal structure
4 is occupied by the vicinal diol of the phytosphingosine chain of α -GC was occupied in
5 the BPGC bound models by a less bulky amide group. This allowed reorientation of the
6 TCR α R95 side chain (R95 α) into the same region, forming a favourable stacking
7 interaction between the guanidinium of the arginine and the amide of the ligand. The
8 guanidinium of R95 α was also sandwiched between the mCD1d residues D284 and
9 D211, salt-bridging with both aspartates. Other interactions stabilizing the predicted
10 BPGC binding orientation were apparent, such as hydrogen bonds between the amide
11 group and residues S207 and T287 of mCD1d, and between the C3 hydroxyl of the
12 phytosphingosine chain and residue T290 of mCD1d. (d) CD1d surface in the region of
13 the modified terminal, colored by electrostatic potential (blue indicates nonpolar and red
14 indicates polar surfaces). The end group forms favourable non-polar contacts with I229,
15 V249, F251, W264, W273, L274, I278 and L281 (residue numbers are based on the
16 mCD1d-fusion protein).

17
18 The final refined structures of **9** and **13** glycolipids after docking showed similar
19 binding modes except for the linker region, as expected (**Fig. 6, inset**). Compared to
20 the corresponding sugar moiety of α -GC C26:0 in the crystal structure, the
21 α -galactopyranosyl group in BPGC analogues was positioned closer to the TCR and
22 slightly shifted (**Fig. 6a**). The lipid chains occupying the A' and F' pockets in the models
23 with bound BPGCs were switched compared to the orientation of α -GC C26:0 in the
24 crystal structure. Thus, the acyl chain of the covalently bound **9** and **13** was positioned
25 in the F' pocket of mCD1d, rather than in the A' pocket as in the case of the
26 noncovalently bound α -GC C26:0 (**Fig. 6a and b**). This binding orientation allowed
27 reorientation of the TCR α R95 side chain (R95 α) to form a favourable stacking

1
2
3 1 interaction between the guanidinium of the arginine and the amide of the ligand, as well
4
5 2 as a number of other stabilizing interactions (**Fig. 6c**). The acyl chains of **9** and **13**
6
7 3 adopted quite similar orientations in the two BPGC models in spite of their different
8
9 4 lengths, linking the diphenylmethanol moiety covalently bound to the side chain of V257
10
11 5 in a mainly non-polar pocket (**Fig. 6d**).
12
13
14
15
16
17

18 7 **Discussion**

19 8 In this study we synthesized a series of benzophenone-modified glycolipids that can be
20
21 9 covalently cross-linked to soluble as well as surface expressed CD1d to generate highly
22
23 10 stable conjugates that activate iNKT cells *in vitro* and *in vivo*. By appending a
24
25 11 photoactivatable benzophenone group to the end of the amide linked acyl chain of
26
27 12 α -GC, we generated a family of BPGCs with varying aliphatic spacer lengths.
28
29 13 Screening for biologic activity using a variety of assays for iNKT cell stimulation showed
30
31 14 that all of these BPGCs could be presented by CD1d, with most experiments showing
32
33 15 **13** to be optimal for iNKT cell stimulation. Using relatively brief and low energy UV
34
35 16 irradiation, all of the BPGCs could be activated to form stable conjugates with purified
36
37 17 CD1d proteins. In addition, UV photoactivation could be shown to stabilize BPGC
38
39 18 interactions with CD1d expressed in living cells. By multiple criteria, UV induced
40
41 19 covalent conjugates of BPGCs retained their interactions with iNKT cell TCRs, and
42
43 20 conjugates in either soluble, surface bound or cell associated forms possessed the
44
45 21 ability to activate cytokine secretion by iNKT cells.
46
47
48
49
50

51 22 Our primary goal in developing BPGCs was to use conjugate formation with
52
53 23 CD1d as a method for improving delivery of iNKT cell activators as potential agents for
54
55 24 immunotherapy. Particularly in the case of cancer immunotherapy, many studies in
56
57
58
59
60

1 mouse models have highlighted the potential for iNKT cell activators to deliver striking
2 anti-cancer effects.^{4c} However, administration of α -GC as a free glycolipid has the
3 potential for dose limiting toxicity, and also leads to the rapid development of a long-
4 lived hyporesponsive state (anergy) that interferes with repeated treatments.^{10, 21} Most
5 likely, these issues contribute to the limited efficacy of free α -GC injections observed so
6 far in early phase clinical trials for cancer in humans.^{9, 22} Approaches to more precisely
7 deliver α -GC to overcome these problems have been developed, including the
8 administration of *ex vivo* glycolipid loaded antigen presenting cells or targeted soluble
9 recombinant CD1d proteins.^{4c, 8a, 8c, 8d} These approaches have shown improved
10 outcomes in animal models, as well as in limited clinical studies in cancer patients^{4c, 6b,}
11 ²³. However, the ability of α -GC to dissociate from these delivery vehicles after *in vivo*
12 injection remains a suboptimal feature. The use of BPGCs to covalently lock the
13 glycolipid onto CD1d in an active configuration, as shown in the current study,
14 represents a method for improving these delivery methods, and achieving more focused
15 and effective immunotherapy without the limitations or toxic effects of systemic α -GC
16 injections.

17 Detailed analysis of the effects of variation in the length of the acyl chain spacer
18 in the BPGCs revealed some interesting and potentially important findings. First, we
19 noted that the **9** and **10** compounds had very low TCR affinity and low stimulatory
20 activity when not covalently linked to CD1d (**Figs. 3f and 4a**), presumably because of
21 their rapid dissociation. However, with conjugate formation these glycolipids showed
22 improved affinity and enhanced iNKT cell stimulation. This suggests that the BPGCs
23 with shorter acyl chains, even if released by some mechanism after conjugation, should

1
2
3 1 be less likely to induce unwanted effects such as iNKT cell anergy or systemic toxicity.
4
5 2 Another notable finding was that **9**, which even after conjugation continued to show a
6
7 3 lower TCR affinity than the other BPGCs, also gave a remarkably biased cytokine
8
9 4 response (i.e., significant IFN- γ levels with no detectable IL-4 or other cytokines) when
10
11 5 injected in the form of a conjugate with soluble CD1d protein (**Fig. 4b**). This type of
12
13 6 “Th1-biased” cytokine response has been repeatedly associated in previous studies
14
15 7 with analogues of α -GC that provide superior anti-tumor responses in mouse models.²⁴
16
17 8 Thus, through alterations in the length of the acyl chain spacer, it should be possible to
18
19 9 tune the responses to BPGC conjugates in terms of affinity and biologic response to
20
21 10 optimize desired therapeutic outcomes.
22
23
24
25

26 11 Our mapping of the site of covalent bond formation in **9** and **13** conjugates
27
28 12 yielded the surprising finding of a single major conjugation site for both glycolipids.
29
30 13 Another surprising aspect of this result was that the specific region of CD1d that was
31
32 14 implicated was located near the base of the F' pocket, which in all CD1d-glycolipid
33
34 15 complexes resolved by X-ray crystallography would be predicted to be in greater
35
36 16 proximity to the sphingoid base than the acyl tail of the glycolipid (**Fig. 5c**).² However,
37
38 17 this apparent switch in the orientation of the two lipid tails of the glycolipid can be readily
39
40 18 accommodated in energetically favorable poses of the glycolipid in molecular models
41
42 19 (**Fig. 6**). Thus, our findings suggest the possibility of greater flexibility in the lipid
43
44 20 binding process of CD1d, which has only been occasionally hinted at in atomic level
45
46 21 structure studies.²⁵ Further structural analyses of CD1d-BPGC conjugates should
47
48 22 enable new types of analyses to expand our understanding of the unique process of
49
50
51
52
53
54
55
56
57
58
59
60

1 glycolipid antigen presentation, as well as opportunities for improving immunotherapies
2 that target iNKT cells.

3 4 **EXPERIMENTAL METHODS**

5
6 **Synthesis and compound characterization.** Full experimental details of the synthesis
7 and characterization of all compounds used in this study are provided in the
8 **Supplementary Information.**

9
10 **Mice.** Female C57BL/6J (B6) mice 6–8 weeks old were obtained from Jackson
11 Laboratories or Taconic and maintained in pathogen-free conditions. All experiments
12 requiring mice were conducted in compliance with institutional guidelines and under an
13 authorization delivered by the Institute of Animal Use and Biosafety Committee at Albert
14 Einstein College of Medicine.

15
16 **Cell lines, clones and hybridomas.** HeLa cells transfected with human CD1d
17 (HeLa.hCD1d) were cultured in DMEM supplemented with 10% FBS, and JAWS II cells
18 were cultured in α -MEM supplemented with 10% FBS and 20 ng/ml murine GM-CSF.
19 Mouse splenocytes were maintained in RPMI with 10% FBS. BMDCs were prepared as
20 described earlier and cultured in RPMI supplemented with 10% FBS. Mouse iNKT
21 hybridoma DN3A4-1.2 was maintained in complete RPMI medium containing 10%
22 de complemented serum.²⁶ Human iNKT clonal HDE3 was clonally expanded by
23 stimulation with PHA-P in the presence of recombinant human IL-2 at 250 IU/ mL ,
24 recombinant human IL-7 at 10 ng/mL and allogeneic PBMCs (irradiated at 5000 rad),

1
2
3 1 and cultures were fed by addition of fresh medium containing IL-7 and IL-2 every 2-3
4
5 2 days.^{8d, 15}
6
7
8
9

10 4 **Recombinant CD1d proteins and monoclonal antibody L363.** Single chain β 2m-
11
12 5 mouse CD1d-hexahistidine (MW ~57 kDa) and human CD1d- β 2m-hexahistidine were
13
14 6 purified from CHO cells stably transfected with respective genes.^{27 15} Single chain
15
16 7 mCD1d- β 2m with a C-terminal single chain immunoglobulin Fv fusion (mCD1d- β 2m-
17
18 8 ScFv, MW ~78 kDa) was produced in transiently transfected HEK cells and purified as
19
20 9 previously described.^{8c, 8d} The ScFv moieties of these proteins were specific for the
21
22 10 human tumor associated antigens CEA or C35, although their specific binding
23
24 11 properties were not relevant to experiments in the current study.
25
26
27

28 12 To determine the affinity of mCD1d-BPGC tetramers for iNKT-cell TCRs, 1×10^4
29
30 13 DN3A4-1.2 cells were stained with a range of concentrations of tetramers loaded with
31
32 14 the different glycolipids to form complexes. Soluble mCD1d proteins were prepared and
33
34 15 biotinylated following published methods with minor modifications.²⁸ Glycolipids were
35
36 16 prepared and loaded onto soluble mCD1d as described in the following section. In
37
38 17 some cases, the loaded mCD1d complexes were converted to covalent conjugates by
39
40 18 exposure to UV irradiation for 60 minutes in solution (400 mJoules/cm²). Formation of
41
42 19 tetramers, equilibrium binding of tetramers to NKT cells, and measurement of binding by
43
44 20 flow cytometry has been previously described in detail.¹⁵
45
46
47
48

49 21 Monoclonal antibody L363, specific for mCD1d with bound α -GC C26:0 and other
50
51 22 related forms of α -GC, has been previously described^{15, 18, 29} The antibody was purified
52
53 23 from supernatants of the cultured hybridoma line, and was biotinylated using sulfo-NHS
54
55
56
57
58
59
60

1 biotinylation kit or fluorescently tagged with Alexa Fluor 647 (Alexa 647 labelling kit,
2 Thermo Fisher). Binding of fluorescently labeled L363 to cells was determined by flow
3 cytometry using an LSR II cytometer (BD Biosciences) and FlowJo software.^{15, 19}

4
5 **CD1d loading and covalent crosslinking.** Glycolipids dissolved in DMSO at 1 mg/ml
6 were diluted to 100 μ M concentration in appropriate volumes of PBS and PBS plus
7 0.1% Triton X-100 to yield final DMSO concentration of 8-10% and 0.05% Triton X-100.
8 Glycolipids were added to CD1d at a molar ratio of 3:1 in PBS plus 0.05% Triton X-100
9 (for *in vitro* applications) or PBS + 0.05% Tween-20 (for *in vivo* applications), and
10 incubated for 12-18 hours for complete loading of the complexes. Loaded complexes
11 were transferred to ultra-low binding microtiter plate wells and cooled on ice. A fixed
12 wavelength UV lamp (Schleicher & Schuell, RAD-FREE long wave UV lamp, $\lambda = 365$
13 nm) was placed directly over wells containing complexes for 1 hour on ice. Resulting
14 conjugates were recovered from the wells and excess glycolipid and detergent was
15 removed using detergent-removal columns (Pierce).

16 An azide-functionalized **13** was employed to determine the efficiency of covalent
17 cross-linking. The azido-**13** conjugates and complexes were covalently coupled to
18 dibenzene-cyclooctyne tetramethylrhodamine (DBCO-TAMRA, Click Chemistry Tools)
19 by Huisgen cycloaddition.¹⁷ The ternary complex thus obtained was denatured using
20 DTT and SDS and run on SDS-PAGE for detection. To determine stability of
21 conjugates, the complexes and conjugates were coated onto high binding 96 well plates
22 and washed with PBS-Tx 0.05% every 12 hours for three days to remove reversibly
23 bound glycolipids. Plates were incubated at room temperature between washes.

1 For detection of mCD1d-glycolipid complexes and conjugates on glycolipid
2 pulsed JAWS II cells, the cells were plated at 5×10^4 cells per well in microtiter plates
3 and cultured with 100 nM of either α -GC C26:0 or **13** for 18 hours, followed by one wash
4 with medium and then UV irradiation if indicated for 30 minutes (~400
5 mJ/cm²). Samples of UV exposed and non-exposed cells were stained with mAb L363
6 coupled with AlexaFluor 647 and analyzed by flow cytometry using an LSR II flow
7 cytometer (BD Biosciences) to determine surface bound glycolipid-CD1d complexes or
8 conjugates (solid black bars), before and after incubation for two days to allow
9 dissociation of glycolipids.

10
11 ***In vitro* and *in vivo* iNKT-cell stimulation assays.** To determine the EC₅₀ of BPGCs,
12 BMDCs from C57BL/6 mice or human CD1d transfected HeLa cells (HeLa.hCD1d) were
13 cultured in microtiter plate wells (5×10^4 BMDC and 1×10^4 HeLa.hCD1d per well), and
14 pulsed with varying BPGC concentrations ranging between 50 μ M and 0.01 nM in 100
15 μ l of culture medium per well for 3 hours at 37 °C. Cells were washed once to remove
16 unbound glycolipid. The iNKT hybridoma DN3A4-1.2 or human iNKT clone HDE3 were
17 then added (5×10^4 cells per well in 0.2 ml medium), and the cultures were maintained
18 for 12 – 18 hours at 37°C. Stimulation was determined by measuring supernatant levels
19 of IL-2 for DN3A4 1.2 or IFN- γ for HDE3 by capture ELISA as described.³⁰ Cytokine
20 response was plotted against dose and EC₅₀ was calculated using the function log
21 agonist against response in Prism software.

22 To determine the serum cytokine levels induced *in vivo* in mice by administration
23 of free glycolipids, glycolipid-loaded mCD1d complexes and conjugates, or *ex vivo*

1 glycolipid loaded JAWS II cells, mice were bled at 2, 10 and 24 hours following i.v.
2 injections and serum samples were prepared. For free glycolipids, mice (3-5 per group)
3 received 4 nanomoles of α -GC C26:0, **9**, **13** or **15**. For comparison of *in vivo* activity of
4 conjugates, complexes and free glycolipids, 30 μ g/mouse of complexes or conjugates or
5 equimolar amounts of free BPGCs (0.4 nanomoles) were injected into mice i.v. Serum
6 cytokine levels were measured by capture ELISA.

7
8 **Mass spectrometry and proteomic analyses.** Tryptic and chymotryptic peptide digest
9 mixtures of native mCD1d or conjugates were analysed either directly by on-line nano-
10 liquid chromatography (nano-LC) electrospray (ES) MS and MS/MS, or subjected to *N*-
11 linked glycan release by PNGase F followed by subdigestion with additional proteases
12 prior to analysis. For detailed method see Supplemental Methods section.

13
14 **Computational molecular modeling and docking studies.** Binding modes of **9** and
15 **13** glycolipids to mCD1d were predicted using the mCD1d/ α -GC/TCR crystal structure
16 with PDB entry code 3HE6, containing V α 14-V β 8.2 iNKT TCR (mouse variable, human
17 constant domains). The crystal structure was prepared using Protein Preparation
18 Wizard tools (Schrödinger software package, version 2016-1). For detailed method see
19 Supplemental Methods section.

20
21 **Statistical analysis.** Results are expressed as mean \pm SEM. Statistical significance
22 between the groups was determined with multiple t tests, one-way-ANOVA or two-way-

1
2
3 1 ANOVA tests with the Bonferroni correction as indicated. All statistical analyses were
4
5 2 done using GraphPad Prism software.
6
7
8 3
9

10 4 **Acknowledgments**

11
12 5 Major funding support was provided by NIH/NIAID grant R01 AI45889 and U01
13
14 6 GM111849 (to SAP). GSB acknowledges support in the form of a Personal Research
15
16
17 7 Chair from Mr. James Bardrick and a Royal Society Wolfson Research Merit Award.
18
19 8 SMH and SJN were supported by Biotechnology and Biological Sciences Research
20
21 9 Council Grant BB/K016164/1. Flow cytometry and recombinant protein production were
22
23 10 supported by core facilities of the Albert Einstein College of Medicine Cancer Center
24
25 11 (NCI grant CA13330). We thank Drs. Alena Donda (Ludwig Cancer Institute) and Amy
26
27 12 Howell (University of Connecticut) for helpful discussions.
28
29
30
31 13

32 14 **Competing financial interests**

33
34
35 15 MZ is an employee of Vaccinex, Inc., which has proprietary interests in iNKT cell-based
36
37 16 immunotherapeutics. SAP is a paid consultant of Vaccinex, Inc. The other authors
38
39 17 declare no competing financial interests.
40
41
42 18
43
44

45 19 **Additional information**

46
47 20 Any supplementary information, chemical compound information and source data are
48
49 21 available in the online version of the paper.
50
51
52 22
53

54 23 **References**

55
56 24
57
58
59
60

1. Brennan, P. J.; Brigl, M.; Brenner, M. B., Invariant natural killer T cells: an innate activation scheme linked to diverse effector functions. *Nature reviews. Immunology* **2013**, *13* (2), 101-17.
2. Rossjohn, J.; Pellicci, D. G.; Patel, O.; Gapin, L.; Godfrey, D. I., Recognition of CD1d-restricted antigens by natural killer T cells. *Nature reviews. Immunology* **2012**, *12* (12), 845-57.
3. Laurent, X.; Bertin, B.; Renault, N.; Farce, A.; Speca, S.; Milhomme, O.; Millet, R.; Desreumaux, P.; Henon, E.; Chavatte, P., Switching invariant natural killer T (iNKT) cell response from anticancerous to anti-inflammatory effect: molecular bases. *J Med Chem* **2014**, *57* (13), 5489-508.
4. (a) Kawano, T.; Cui, J.; Koezuka, Y.; Toura, I.; Kaneko, Y.; Motoki, K.; Ueno, H.; Nakagawa, R.; Sato, H.; Kondo, E., et al., CD1d-restricted and TCR-mediated activation of valpha14 NKT cells by glycosylceramides. *Science* **1997**, *278* (5343), 1626-9; (b) Motoki, K.; Morita, M.; Kobayashi, E.; Uchida, T.; Akimoto, K.; Fukushima, H.; Koezuka, Y., Immunostimulatory and antitumor activities of monoglycosylceramides having various sugar moieties. *Biological & pharmaceutical bulletin* **1995**, *18* (11), 1487-91; (c) Nair, S.; Dhodapkar, M. V., Natural Killer T Cells in Cancer Immunotherapy. *Front Immunol* **2017**, *8*, 1178.
5. (a) Cerundolo, V.; Salio, M., Harnessing NKT cells for therapeutic applications. *Curr Top Microbiol Immunol* **2007**, *314*, 325-40; (b) Cerundolo, V.; Silk, J. D.; Masri, S. H.; Salio, M., Harnessing invariant NKT cells in vaccination strategies. *Nature reviews. Immunology* **2009**, *9* (1), 28-38.
6. (a) Kharkwal, S. S.; Arora, P.; Porcelli, S. A., Glycolipid activators of invariant NKT cells as vaccine adjuvants. *Immunogenetics* **2016**, *68* (8), 597-610; (b) Exley, M. A.; Nakayama, T., NKT-cell-based immunotherapies in clinical trials. *Clin Immunol* **2011**, *140* (2), 117-8.
7. (a) Birkholz, A. M.; Kronenberg, M., Antigen specificity of invariant natural killer T-cells. *Biomed J* **2015**, *38* (6), 470-83; (b) Carreno, L. J.; Saavedra-Avila, N. A.; Porcelli, S. A., Synthetic glycolipid activators of natural killer T cells as immunotherapeutic agents. *Clin Transl Immunology* **2016**, *5* (4), e69.
8. (a) Fujii, S.; Shimizu, K.; Kronenberg, M.; Steinman, R. M., Prolonged IFN-gamma-producing NKT response induced with alpha-galactosylceramide-loaded DCs. *Nature immunology* **2002**, *3* (9), 867-74; (b) Kimura, H.; Matsui, Y.; Ishikawa, A.; Nakajima, T.; Yoshino, M.; Sakairi, Y., Randomized controlled phase III trial of adjuvant chemo-immunotherapy with activated killer T cells and dendritic cells in patients with resected primary lung cancer. *Cancer Immunol Immunother* **2015**, *64* (1), 51-9; (c) Stirnemann, K.; Romero, J. F.; Baldi, L.; Robert, B.; Cesson, V.; Besra, G. S.; Zauderer, M.; Wurm, F.; Corradin, G.; Mach, J. P., et al., Sustained activation and tumor targeting of NKT cells using a CD1d-anti-HER2-scFv fusion protein induce antitumor effects in mice. *The Journal of clinical investigation* **2008**, *118* (3), 994-1005; (d) Corgnac, S.; Perret, R.; Derre, L.; Zhang, L.; Stirnemann, K.; Zauderer, M.; Speiser, D. E.; Mach, J. P.; Romero, P.; Donda, A., CD1d-antibody fusion proteins target iNKT cells to the tumor and trigger long-term therapeutic responses. *Cancer Immunol Immunother* **2013**, *62* (4), 747-60.
9. Wolf, B. J.; Choi, J. E.; Exley, M. A., Novel Approaches to Exploiting Invariant NKT Cells in Cancer Immunotherapy. *Front Immunol* **2018**, *9*, 384.

- 1
2
3 10. Parekh, V. V.; Wilson, M. T.; Olivares-Villagomez, D.; Singh, A. K.; Wu, L.;
4 Wang, C. R.; Joyce, S.; Van Kaer, L., Glycolipid antigen induces long-term natural killer
5 T cell anergy in mice. *The Journal of clinical investigation* **2005**, *115* (9), 2572-83.
- 6 11. (a) Naidenko, O. V.; Maher, J. K.; Ernst, W. A.; Sakai, T.; Modlin, R. L.;
7 Kronenberg, M., Binding and antigen presentation of ceramide-containing glycolipids by
8 soluble mouse and human CD1d molecules. *J Exp Med* **1999**, *190* (8), 1069-80; (b)
9 Sidobre, S.; Hammond, K. J.; Benazet-Sidobre, L.; Maltsev, S. D.; Richardson, S. K.;
10 Ndonye, R. M.; Howell, A. R.; Sakai, T.; Besra, G. S.; Porcelli, S. A., et al., The T cell
11 antigen receptor expressed by Valpha14i NKT cells has a unique mode of
12 glycosphingolipid antigen recognition. *Proceedings of the National Academy of
13 Sciences of the United States of America* **2004**, *101* (33), 12254-9; (c) van den Elzen,
14 P.; Garg, S.; Leon, L.; Brigl, M.; Leadbetter, E. A.; Gumperz, J. E.; Dascher, C. C.;
15 Cheng, T. Y.; Sacks, F. M.; Illarionov, P. A., et al., Apolipoprotein-mediated pathways of
16 lipid antigen presentation. *Nature* **2005**, *437* (7060), 906-10; (d) Yuan, W.; Qi, X.;
17 Tsang, P.; Kang, S. J.; Illarionov, P. A.; Besra, G. S.; Gumperz, J.; Cresswell, P.,
18 Saposin B is the dominant saposin that facilitates lipid binding to human CD1d
19 molecules. *Proceedings of the National Academy of Sciences of the United States of
20 America* **2007**, *104* (13), 5551-6.
- 21 12. (a) Gao, B.; Radaeva, S.; Park, O., Liver natural killer and natural killer T cells:
22 immunobiology and emerging roles in liver diseases. *Journal of leukocyte biology* **2009**,
23 *86* (3), 513-28; (b) Szabo, P. A.; Rudak, P. T.; Choi, J.; Xu, S. X.; Schaub, R.; Singh, B.;
24 McCormick, J. K.; Haeryfar, S. M. M., Invariant Natural Killer T Cells Are Pathogenic in
25 the HLA-DR4-Transgenic Humanized Mouse Model of Toxic Shock Syndrome and Can
26 Be Targeted to Reduce Morbidity. *J Infect Dis* **2017**, *215* (5), 824-829.
- 27 13. (a) Koch, M.; Stronge, V. S.; Shepherd, D.; Gadola, S. D.; Mathew, B.; Ritter, G.;
28 Fersht, A. R.; Besra, G. S.; Schmidt, R. R.; Jones, E. Y., et al., The crystal structure of
29 human CD1d with and without alpha-galactosylceramide. *Nature immunology* **2005**, *6*
30 (8), 819-26; (b) Zeng, Z.; Castano, A. R.; Segelke, B. W.; Stura, E. A.; Peterson, P. A.;
31 Wilson, I. A., Crystal structure of mouse CD1: An MHC-like fold with a large
32 hydrophobic binding groove. *Science* **1997**, *277* (5324), 339-45.
- 33 14. Mitchell, D.; Lukeman, M.; Lehnher, D.; Wan, P., Formal intramolecular
34 photoredox chemistry of meta-substituted benzophenones. *Org Lett* **2005**, *7* (15), 3387-
35 9.
- 36 15. Im, J. S.; Arora, P.; Bricard, G.; Molano, A.; Venkataswamy, M. M.; Baine, I.;
37 Jerud, E. S.; Goldberg, M. F.; Baena, A.; Yu, K. O., et al., Kinetics and cellular site of
38 glycolipid loading control the outcome of natural killer T cell activation. *Immunity* **2009**,
39 *30* (6), 888-98.
- 40 16. Bricard, G.; Venkataswamy, M. M.; Yu, K. O.; Im, J. S.; Ndonye, R. M.; Howell,
41 A. R.; Veerapen, N.; Illarionov, P. A.; Besra, G. S.; Li, Q., et al., Alpha-
42 galactosylceramide analogs with weak agonist activity for human iNKT cells define new
43 candidate anti-inflammatory agents. *PLoS One* **2010**, *5* (12), e14374.
- 44 17. Jeon, J.; Kang, J. A.; Shim, H. E.; Nam, Y. R.; Yoon, S.; Kim, H. R.; Lee, D. E.;
45 Park, S. H., Efficient method for iodine radioisotope labeling of cyclooctyne-containing
46 molecules using strain-promoted copper-free click reaction. *Bioorg Med Chem* **2015**, *23*
47 (13), 3303-8.

- 1
2
3 18. Yu, K. O.; Im, J. S.; Illarionov, P. A.; Ndonge, R. M.; Howell, A. R.; Besra, G. S.;
4 2 Porcelli, S. A., Production and characterization of monoclonal antibodies against
5 3 complexes of the NKT cell ligand alpha-galactosylceramide bound to mouse CD1d.
6 4 *Journal of immunological methods* **2007**, *323* (1), 11-23.
- 7 5 19. Arora, P.; Baena, A.; Yu, K. O.; Saini, N. K.; Kharkwal, S. S.; Goldberg, M. F.;
8 6 Kunnath-Velayudhan, S.; Carreno, L. J.; Venkataswamy, M. M.; Kim, J., et al., A single
9 7 subset of dendritic cells controls the cytokine bias of natural killer T cell responses to
10 8 diverse glycolipid antigens. *Immunity* **2014**, *40* (1), 105-16.
- 11 9 20. (a) Thakur, M. S.; Khurana, A.; Kronenberg, M.; Howell, A. R., Synthesis of a 2"-
12 10 deoxy-beta-GalCer. *Molecules* **2014**, *19* (7), 10090-102; (b) Arora, P.; Kharkwal, S. S.;
13 11 Ng, T. W.; Kunnath-Velayudhan, S.; Saini, N. K.; Johndrow, C. T.; Chang, Y. T.; Besra,
14 12 G. S.; Porcelli, S. A., Endocytic pH regulates cell surface localization of glycolipid
15 13 antigen loaded CD1d complexes. *Chemistry and physics of lipids* **2015**, *191*, 75-83; (c)
16 14 Huang, J. R.; Tsai, Y. C.; Chang, Y. J.; Wu, J. C.; Hung, J. T.; Lin, K. H.; Wong, C. H.;
17 15 Yu, A. L., alpha-Galactosylceramide but not phenyl-glycolipids induced NKT cell anergy
18 16 and IL-33-mediated myeloid-derived suppressor cell accumulation via upregulation of
19 17 *egr2/3*. *Journal of immunology* **2014**, *192* (4), 1972-81.
- 20 18 21. Wingender, G.; Birkholz, A. M.; Sag, D.; Farber, E.; Chitale, S.; Howell, A. R.;
21 19 Kronenberg, M., Selective Conditions Are Required for the Induction of Invariant NKT
22 20 Cell Hyporesponsiveness by Antigenic Stimulation. *J Immunol* **2015**, *195* (8), 3838-48.
- 23 21 22. Giaccone, G.; Punt, C. J.; Ando, Y.; Ruijter, R.; Nishi, N.; Peters, M.; von
24 22 Blomberg, B. M.; Scheper, R. J.; van der Vliet, H. J.; van den Eertwegh, A. J., et al., A
25 23 phase I study of the natural killer T-cell ligand alpha-galactosylceramide (KRN7000) in
26 24 patients with solid tumors. *Clinical cancer research : an official journal of the American*
27 25 *Association for Cancer Research* **2002**, *8* (12), 3702-9.
- 28 26 23. (a) Ishikawa, A.; Motohashi, S.; Ishikawa, E.; Fuchida, H.; Higashino, K.; Otsuji,
29 27 M.; Iizasa, T.; Nakayama, T.; Taniguchi, M.; Fujisawa, T., A phase I study of alpha-
30 28 galactosylceramide (KRN7000)-pulsed dendritic cells in patients with advanced and
31 29 recurrent non-small cell lung cancer. *Clinical cancer research : an official journal of the*
32 30 *American Association for Cancer Research* **2005**, *11* (5), 1910-7; (b) Kunii, N.;
33 31 Horiguchi, S.; Motohashi, S.; Yamamoto, H.; Ueno, N.; Yamamoto, S.; Sakurai, D.;
34 32 Taniguchi, M.; Nakayama, T.; Okamoto, Y., Combination therapy of in vitro-expanded
35 33 natural killer T cells and alpha-galactosylceramide-pulsed antigen-presenting cells in
36 34 patients with recurrent head and neck carcinoma. *Cancer science* **2009**, *100* (6), 1092-
37 35 8.
- 38 36 24. (a) Schmieg, J.; Yang, G.; Franck, R. W.; Tsuji, M., Superior protection against
39 37 malaria and melanoma metastases by a C-glycoside analogue of the natural killer T cell
40 38 ligand [alpha]-galactosylceramide. *J. Exp. Med.* **2003**, *198*, 1631-1641; (b) Aspeslagh,
41 39 S.; Nemcovic, M.; Pauwels, N.; Venken, K.; Wang, J.; Van Calenbergh, S.; Zajonc, D.
42 40 M.; Elewaut, D., Enhanced TCR footprint by a novel glycolipid increases NKT-
43 41 dependent tumor protection. *Journal of immunology* **2013**, *191* (6), 2916-25.
- 44 42 25. Girardi, E.; Yu, E. D.; Li, Y.; Tarumoto, N.; Pei, B.; Wang, J.; Illarionov, P.; Kinjo,
45 43 Y.; Kronenberg, M.; Zajonc, D. M., Unique interplay between sugar and lipid in
46 44 determining the antigenic potency of bacterial antigens for NKT cells. *PLoS Biol* **2011**, *9*
47 45 (11), e1001189.

- 1
2
3 1 26. Exley, M.; Garcia, J.; Balk, S. P.; Porcelli, S., Requirements for CD1d recognition
4 2 by human invariant Valpha24+ CD4-CD8- T cells. *J Exp Med* **1997**, *186* (1), 109-20.
5 3 27. Khurana, A.; Kronenberg, M., A method for production of recombinant mCD1d
6 4 protein in insect cells. *J Vis Exp* **2007**, (10), 556.
7 5 28. Im, J. S.; Yu, K. O.; Illarionov, P. A.; LeClair, K. P.; Storey, J. R.; Kennedy, M.
8 6 W.; Besra, G. S.; Porcelli, S. A., Direct measurement of antigen binding properties of
9 7 CD1 proteins using fluorescent lipid probes. *The Journal of biological chemistry* **2004**,
10 8 *279* (1), 299-310.
11 9 29. Arora, P.; Venkataswamy, M. M.; Baena, A.; Bricard, G.; Li, Q.; Veerapen, N.;
12 10 Ndonye, R.; Park, J. J.; Lee, J. H.; Seo, K. C., et al., A rapid fluorescence-based assay
13 11 for classification of iNKT cell activating glycolipids. *Journal of the American Chemical*
14 12 *Society* **2011**, *133* (14), 5198-201.
15 13 30. Jervis, P. J.; Veerapen, N.; Bricard, G.; Cox, L. R.; Porcelli, S. A.; Besra, G. S.,
16 14 Synthesis and biological activity of alpha-glucosyl C24:0 and C20:2 ceramides. *Bioorg*
17 15 *Med Chem Lett* **2010**, *20* (12), 3475-8.

16

17

18

19

20

21

22

23

24

25

26

27

1

2 For Table of Contents Only

